

Supporting Information for:

**Regulating the spin state of single Fe Atom enhances  
photocatalytic nitrogen reduction in Fe-doped BiOBr: insights  
from theoretical studies**

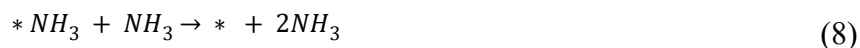
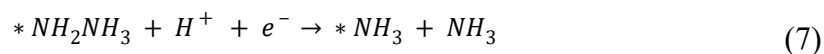
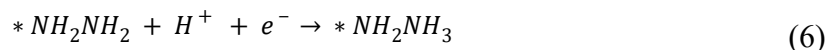
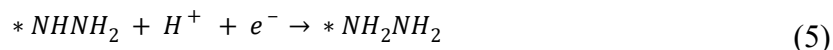
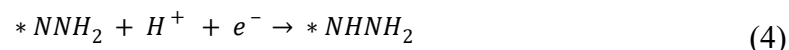
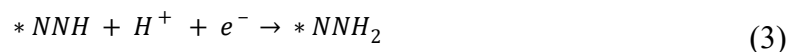
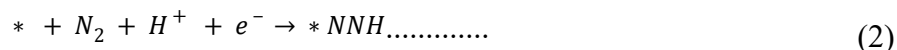
Zhanjin Wang,<sup>†</sup> Xiao Han,<sup>†</sup> Jinlu He<sup>\*</sup>

*College of Chemistry and Chemical Engineering, Inner Mongolia University, Hohhot  
010021, PR China*

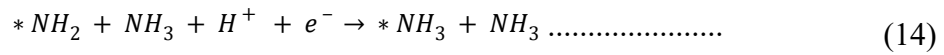
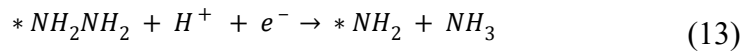
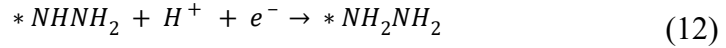
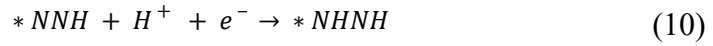
**Theoretical Calculation Details**

The nitrogen reduction reaction (NRR) pathways were calculated according the following equations (2)–(15), the \* denotes the surface of catalysts.<sup>1</sup>

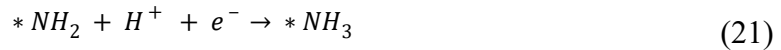
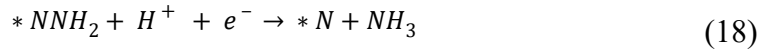
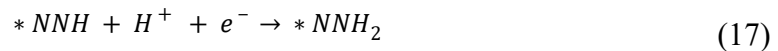
Enzymatic mechanism:



Alternating mechanism:



Distal mechanism:



The Gibbs free energy,  $G$ , was computed according to the equation (8) as follows:<sup>2</sup>

$$G = E + E_{ZPE} - TS - eU \quad (23)$$

In the above equation,  $E$ ,  $E_{ZPE}$ , and  $S$  represents the single point energy, zero point energy and entropy of intermediates for NRR, respectively. The  $U$  is the potential versus standard hydrogen electrode. The temperature is set to 298.15 K.

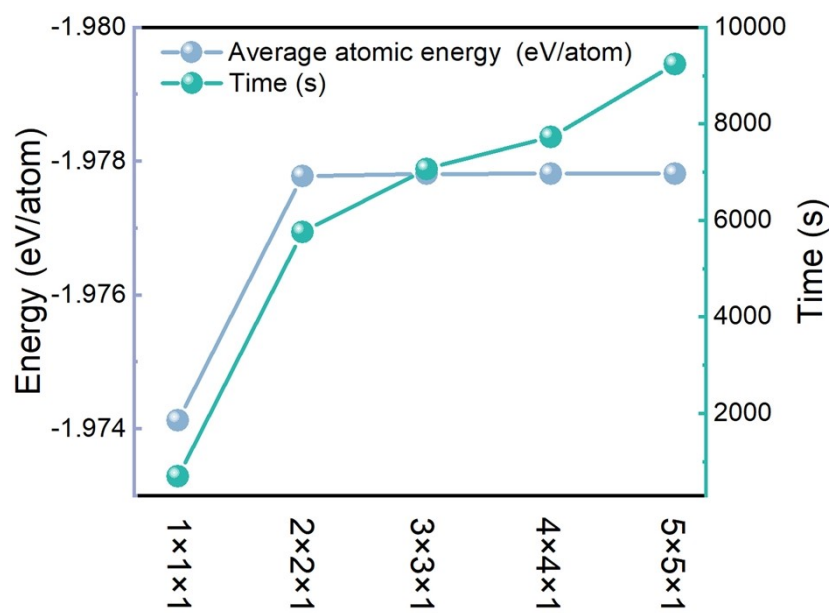


**Fig. S1.** Convergence test of k-points meshes.

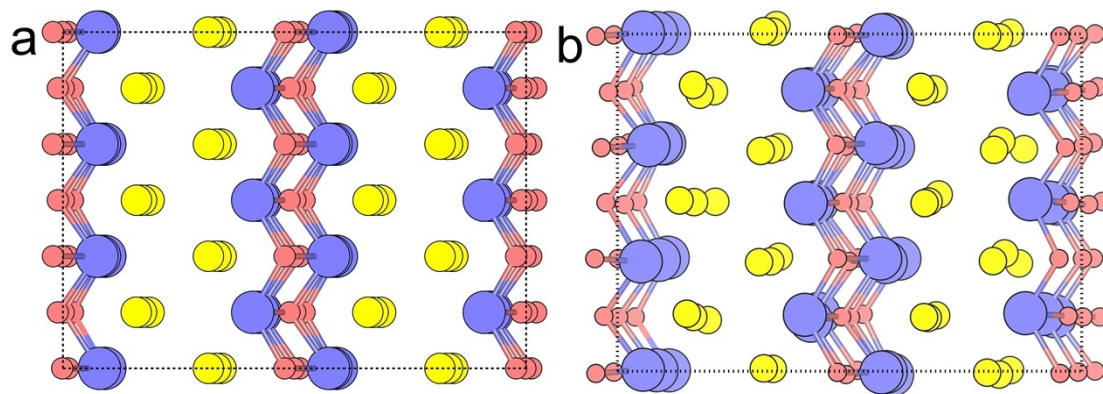


**Fig. S2.** Geometries of pristine BiOBr system at (a) 0 K and (b) 300K. The blue, light red, and yellow spheres denote Bi, O, and Br atoms, respectively.

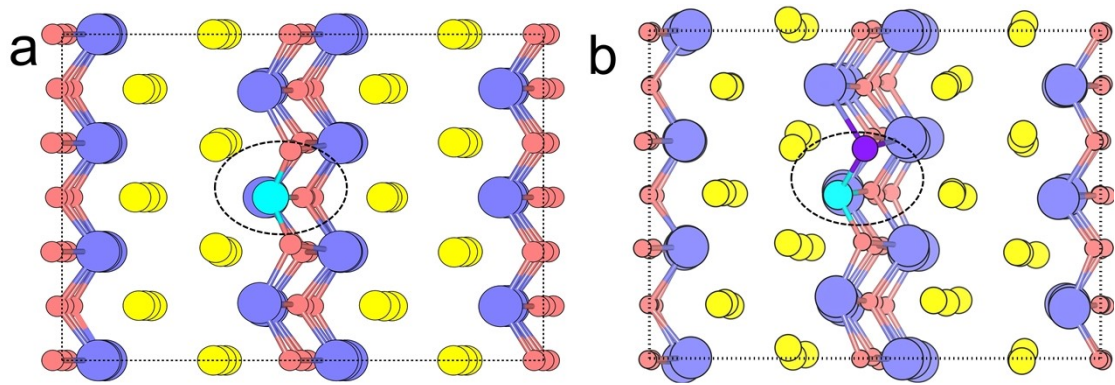


**Fig. S3.** Representative geometries of MD trajectories for (a) Fe-doped and (b) FeP-doped BiOBr systems. The blue, light red, yellow, cyan and purple balls represent Bi, O, Br, Fe and P atoms, respectively.

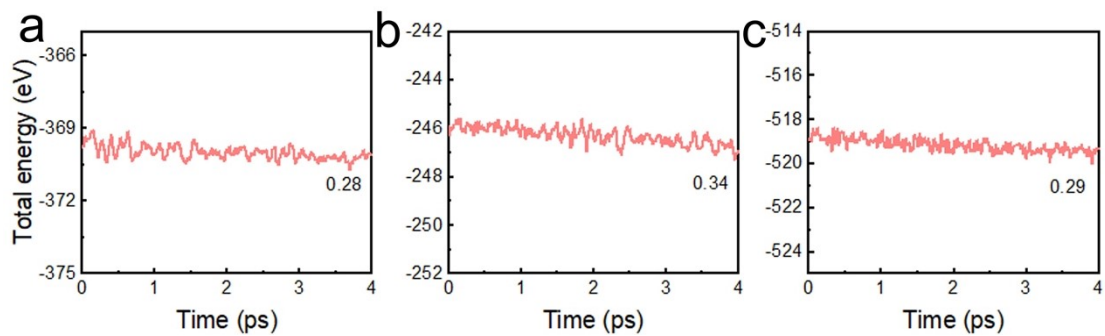


**Fig. S4.** Evolution of total energies during the MD in (a) pristine BiOBr, (a) Fe-doped, and (b) FeP-doped BiOBr systems. The data represent the canonically averaged standard deviations of the total energies.

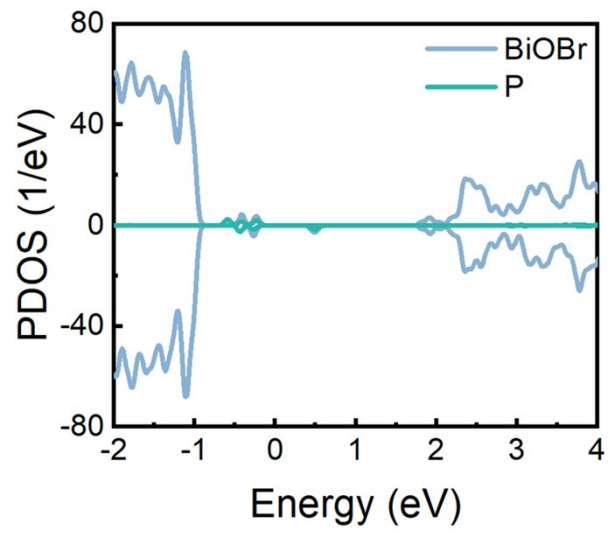


**Fig. S5.** Projected density of states (PDOS) of P doped BiOBr. The Fermi level is set to zero.

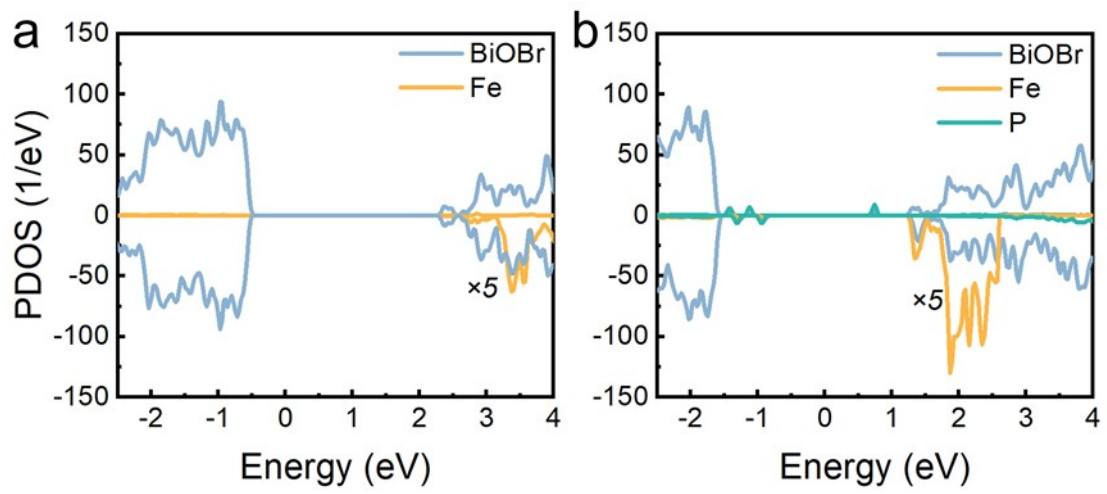


**Fig. S6.** Projected density of states (PDOS) (a) Fe-doped and (b) FeP-doped BiOBr systems calculated using the HSE06 functional. The Fermi level is set to zero.



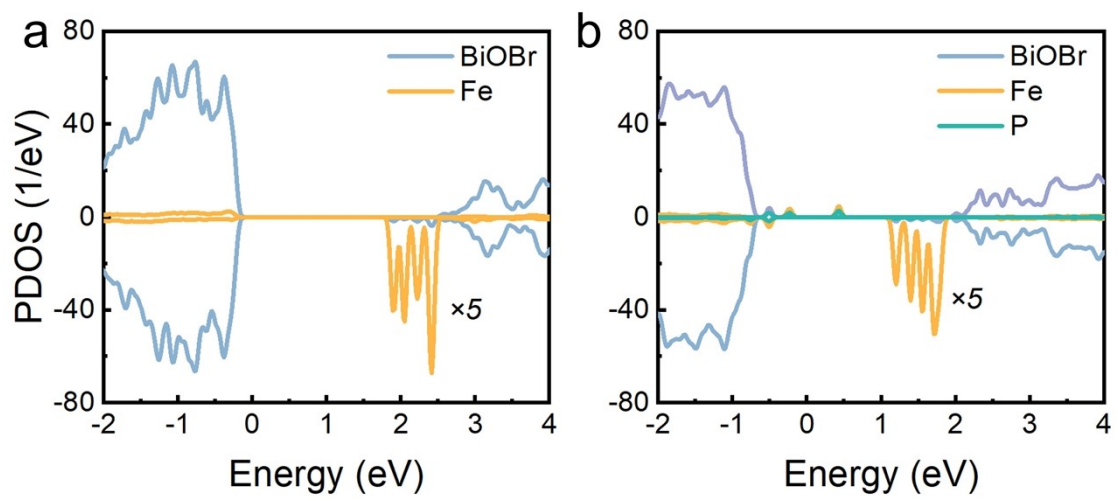


**Fig. S7.** Projected density of states (PDOS) of (a) Fe-doped and (b) FeP-doped BiOBr systems calculated using  $3 \times 3 \times 1$  k-points. The Fermi level is set to zero.

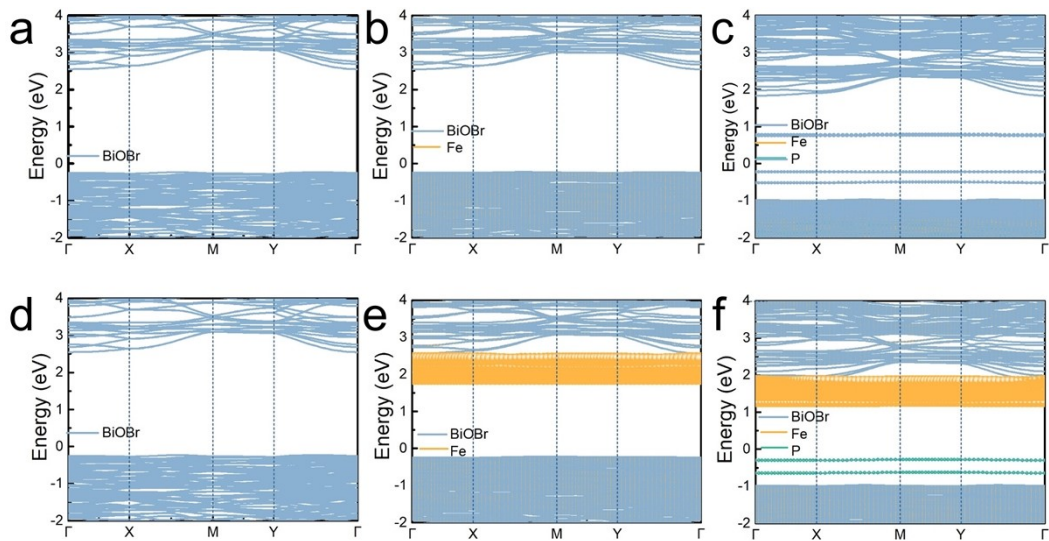


**Fig. S8.** Spin-up (top panel) and spin-down (bottom panel) band structures of (a, d) pristine, (b, e) Fe-doped, and (c, f) FeP-doped BiOBr systems. The Fermi level is set to zero.

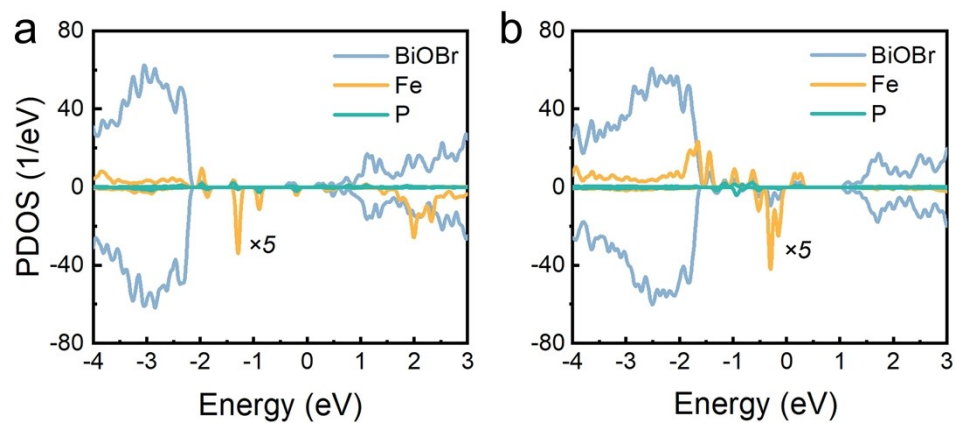


**Fig. S9.** Projected density of states (PDOS) of (a) FeP<sub>2</sub> and (b) FeP<sub>3</sub> doped BiOBr systems. The Fermi level is set to zero.

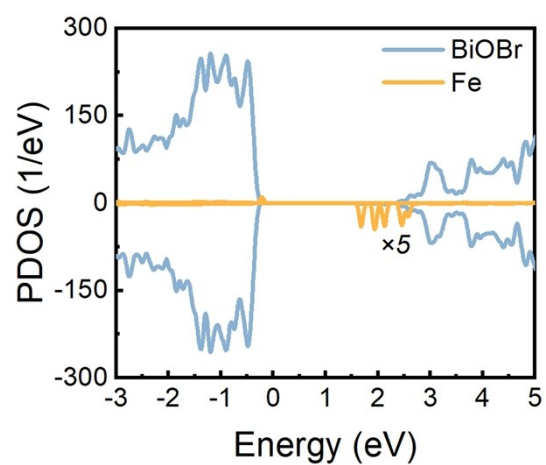


**Fig. S10.** Projected density of states (PDOS) of Fe-doped  $4 \times 4 \times 1$  BiOBr supercell. The Fermi level is set to zero.

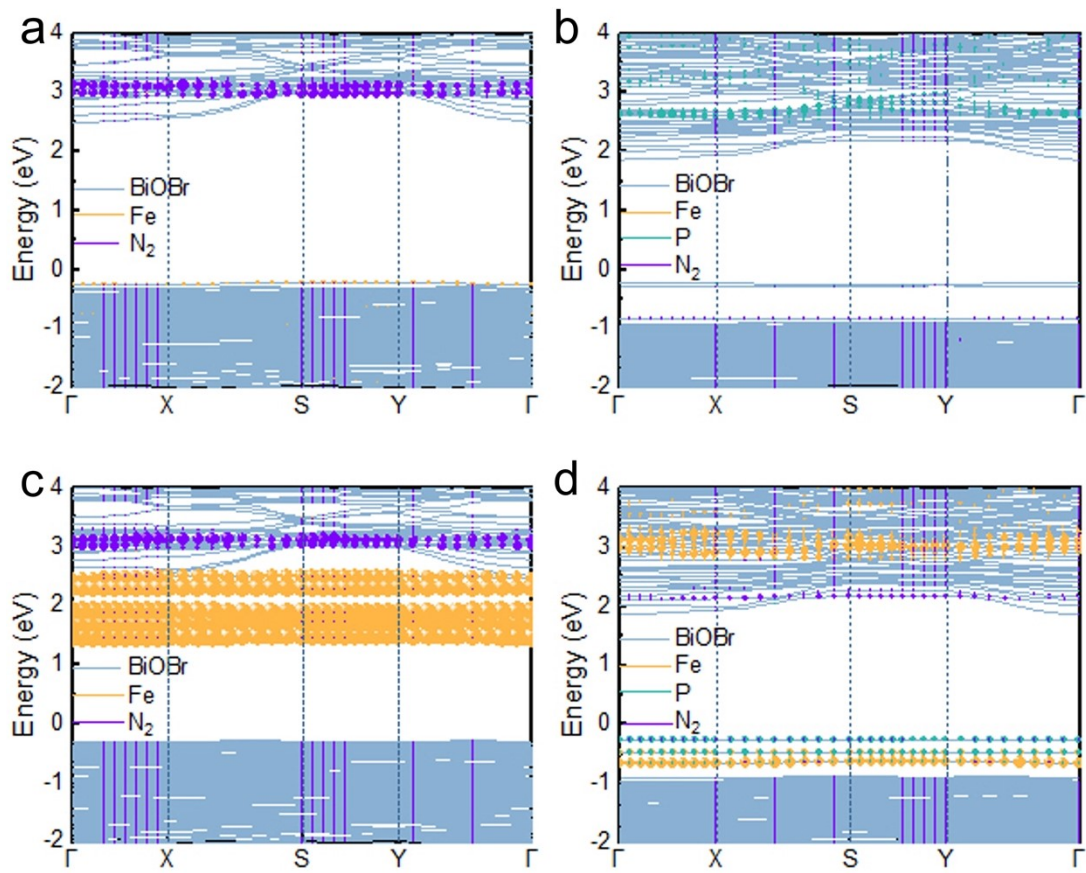


**Fig. S11.** Spin-up (top panel) and spin-down (bottom panel) band structures of nitrogen adsorbed (a, b) Fe-doped and (c, d) FeP-doped BiOBr systems. The Fermi level is set to zero.

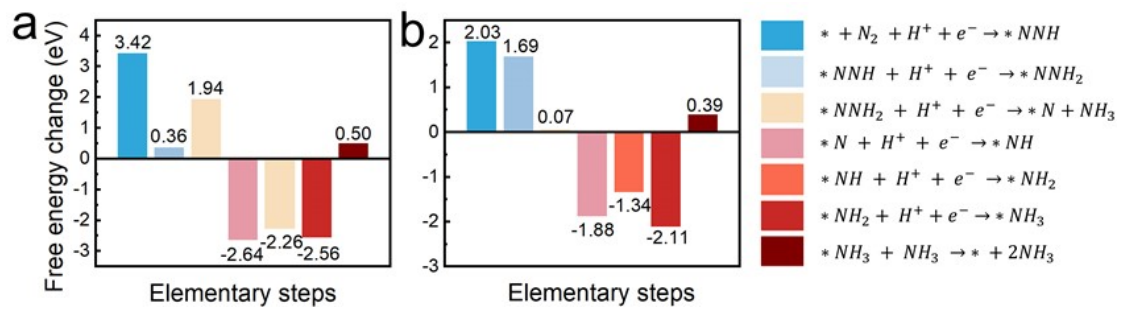


**Fig. S12.** Free energy change for elementary steps along the distal pathways for NRR

in (a) Fe-doped and (b) FeP-doped BiOBr systems.

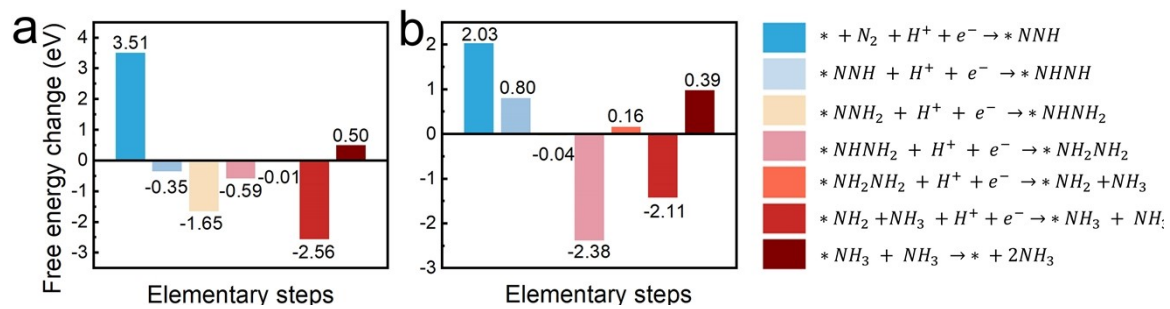


**Fig. S13.** Free energy change for elementary steps along the alternating pathways for NRR in (a) Fe-doped and (b) FeP-doped BiOBr systems.

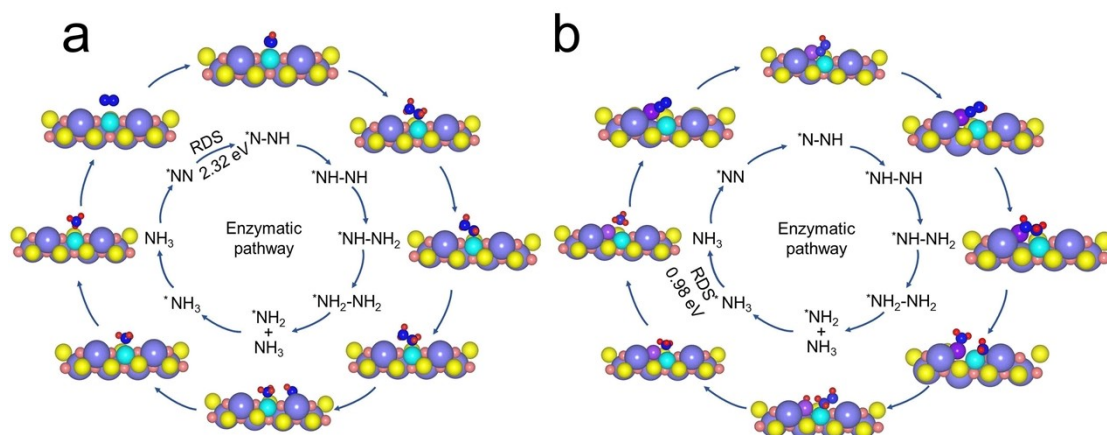


**Fig. S14.** Configurations of the intermediate in the enzymatic pathway for NRR in (a) Fe-doped and (b) FeP-doped BiOBr systems.



## References

- 1 H. D. Shen, M. M. Yang, L. D. Hao, J. R. Wang, J. Strunk and Z. Y. Sun, *Nano Res.*, 2022, **15**, 2773-2809.
- 2 K. Gao, C. Zhang, H. Zhu, J. Xia, J. Chen, F. Xie, X. Zhao, Z. Tang and X. Wang, *Chem. Eur. J.*, 2023, **29**, e202300616.